The Cryosphere Discuss., 8, 121–147, 2014
www.the-cryosphere-discuss.net/8/121/2014/
doi:10.5194/tcd-8-121-2014

The Cryosphere Discussions
Open Access

Physical controls on the storage of methane in landfast sea ice

J. Zhou[1,2], J.-L. Tison[1], G. Carnat[1], N.-X. Geilfus[3], and B. Delille[2]

[1]Laboratoire de glaciologie, DSTE, Université Libre de Bruxelles, Brussels, Belgium
[2]Unité d'Océanographie chimique, MARE, Université de Liège, Liège, Belgium
[3]Arctic Research Center, Aarhus University, Aarhus, Denmark

Received: 13 November 2013 – Accepted: 16 December 2013 – Published: 6 January 2014

Correspondence to: J. Zhou (jiayzhou@ulb.ac.be)

Published by Copernicus Publications on behalf of the European Geosciences Union.

Abstract

We report on methane (CH_4) dynamics in landfast sea ice, brine and under-ice seawater at Barrow in 2009. The CH_4 concentrations in under-ice water ranged between 25.9 and 116.4 nmol L_{sw}^{-1}, indicating a superaturation of 700 to 3100 % relative to the atmosphere. In comparison, the CH_4 concentrations in ice, ranged between 3.4 and 17.2 nmol L_{ice}^{-1}, and the deduced CH_4 concentrations in brine, between 13.2 and 677.7 nmol L_{br}^{-1}. We investigated on the processes explaining the difference in CH_4 concentrations between sea ice, brine and the under-ice water, and suggest that two physical processes regulated the storage of CH_4 in sea ice: bubble formation and sea ice permeability. Gas bubble formation from solubility changes had favoured the accumulation of CH_4 in the ice at the beginning of ice growth. CH_4 retention in sea ice was then twice as efficient as that of salt; this also explains the overall higher CH_4 concentrations in brine than in the under-ice water. As sea ice thickened, gas bubble formation became less efficient so that CH_4 was then mainly trapped in the dissolved state. The increase of sea ice permeability during ice melt marks the end of CH_4 storage.

1 Introduction

Methane (CH_4) is a long-lived greenhouse gas (LLGHGs) (Forster et al., 2007). Its concentration in the atmosphere is much lower than that of its oxidation product (CO_2) (1.8 ppm vs. 390 ppm, respectively) (http://www.esrl.noaa.gov/gmd/aggi/). However, since CH_4 global warming potential is 21 times higher than that of CO_2 (Lelieveld et al., 1998), it accounts for 20 % of the global radiative forcing of LLGHGs (Forster et al., 2007).

The marine system contributes 0.25 % to 3.6 % of the global tropospheric CH_4 input, which ranges between 503 Tg CH_4 yr^{-1} and 610 Tg CH_4 yr^{-1} (see Forster et al. (2007) and references therein). 75 % of the marine contribution is from coastal regions (Bange et al., 1994). CH_4 supersaturation relative to the atmosphere in estuaries (Borges and

TCD
8, 121–147, 2014

Abril, 2011; Upstill-Goddard et al., 2000) and coastal shelves (Kvenvolden et al., 1993; Savvichev et al., 2004; Shakhova et al., 2005; Shakhova et al., 2010) are indeed larger to that in the open ocean (Bates et al., 1996; Damm et al., 2010; Damm et al., 2008; Damm et al., 2007).

Methanogenesis in sub-marine sediments is thought to be the main process causing CH_4 efflux in the Arctic shelf regions. Nonetheless, other sources could also be significant: CH_4 seepage from coastal ice-complex deposits (Romanovskii et al., 2000) and from the deeper seabeds (Judd, 2004), and CH_4 dissociation in the shallow hydrates (Reagan and Moridis, 2008; Westbrook et al., 2009). Recently, aerobic CH_4 production in the water column related to DMSP degradation was reported in the central Arctic (Damm et al., 2010), tropical upwelling areas (Florez-Leiva et al., 2013) and tropical oligotrophic areas (Zindler et al., 2012). However, the significance of such a process over the Arctic shelf still needs to be assessed.

Ongoing global warming is likely to affect the various sources of CH_4 cited above, with positive feedback on the climate. Indeed, increase in sea temperature should increase methanotrophic activities, leading to a more efficient conversion of organic matter to CH_4 (Zeikus and Winfrey, 1976). In addition, the induced seawater stratification is likely to change the nutrients ratio, which favours aerobic CH_4 production (Karl et al., 2008). Moreover, warmer seawater is likely to weaken the coastal ice-complex (including sub-sea permafrost) (Lawrence et al., 2008) and to displace the gas hydrate stability zones (GHSZ) (Reagan and Moridis, 2008), increasing gas seepage. Significant CH_4 escape has been recently detected via acoustic surveys along Spitsbergen continental margin (Westbrook et al., 2009), suggesting that changes in the CH_4 storage system are ongoing. Since CH_4 has a high global warming potential, its release will enhance the global warming, which in turn will enhance methanotroph activities and gas seepages. This positive feedback contributed to rapid and significant climate warming in the past (Kennett et al., 2000; Nisbet, 2002).

Understanding the current CH_4 budget is thus important to better simulate future climate scenarios. Many CH_4 measurements have been carried out in sediments and

TCD
8, 121–147, 2014

seawater throughout the coastal Arctic areas (Kvenvolden et al., 1993; Savvichev et al., 2004; Shakhova et al., 2005; Shakhova et al., 2010). These observations have led to speculations about potential CH_4 accumulation (Shakhova et al., 2010) and/or oxidation (Kitidis et al., 2010) under the sea ice cover. Other studies further brought forward the role of sea ice in the exchange of CH_4 between seawater and the atmosphere (He et al., 2013; Kort et al., 2012). However, to the best of our knowledge, no study has yet discussed the physical controls on the storage of CH_4 in sea ice and its exchange at the atmosphere–ice–ocean interfaces. For instance, CH_4 mixing ratio up to 11 000 ppmV have been measured in sea ice bubbles (Shakhova et al., 2010), but the mechanisms leading to the incorporation of those gas bubbles within the ice have not been discussed. Similarly, He et al. (2013) suggested CH_4 consumption in the ice, based on their CH_4 fluxes above sea ice. However, they did not discuss the impact of sea ice permeability or ice melt on their results, although these parameters have been shown to affect other gas dynamics in sea ice (see e.g., Loose et al. (2009) for O_2 and SF_6, Geilfus et al. (2012) and Nomura et al. (2010) for CO_2 and Zhou et al. (2013) for Ar). Therefore, we felt it necessary to highlight the physical controls on CH_4 dynamics in sea ice, from ice growth to ice melt. We have done this by investigating the annual evolution of CH_4 concentrations ($[CH_4]$) in sea ice, in parallel with sea ice physical properties and $[CH_4]$ in seawater. To the best of our knowledge, we report here the first detailed time series of $[CH_4]$ in sea ice across seasons.

2 Material and methods

2.1 Study site and physical framework

Sea ice and under-ice seawater samples were collected during a field survey in the Chukchi Sea near Barrow (Alaska) (Fig. 1), from January through June 2009. The sampling was performed on level first-year landfast sea ice, within a square of 50 by 50 m. The north-eastern corner of the square was located at 71°22.013′ N,

TCD
8, 121–147, 2014

156°32.447′ W. Seawater depth at the location was about 6.5 m (http://seaice.alaska.edu/gi/observatories/barrow_sealevel). Ice cores were extracted and stored at −30 °C in the dark to prevent brine drainage and to limit biological activity. All of the analyses were completed within the following year. A complete physical framework of the present study is presented and discussed in Zhou et al. (2013). We have selected 6 sampling events to illustrate the evolution of [CH_4] at our location: one in the winter (BRW2; 3 February), 4 in early spring (BRW4, BRW5, BRW6 and BRW7; corresponding to 31 March, 3 April, 7 April and 10 April, respectively), and the final one in late spring (BRW10; 5 June). The first 5 sampling events occurred during ice growth, the last one during ice decay.

2.2 CH_4 in seawater

[CH_4] in seawater were determined by gas chromatography (GC) with flame ionization detection (SRI 8610C GC-FID) (Skoog et al., 1997), after creating a 30 mL headspace with N_2 in 70 mL glass serum bottles, following the procedure described by Abril and Iversen (2002). After creating the N_2 headspace, samples were vigorously shaken for 20 min and were placed in a thermostatic bath overnight at −1.6 °C. The following day, the samples were shaken again for 20 min before starting the GC analysis. CH_4 : CO_2 : N_2 mixtures (Air Liquide, Belgium) of 1, 10 and 30 ppm CH_4 were used as standards. The concentrations were then computed using the CH_4 solubility coefficient given by Yamamoto et al. (1976). The accuracy of the measurements was 1 %.

We calculated the solubility of CH_4 in seawater that is in equilibrium with the atmosphere, following Wiesenburg and Guinasso (1979). The ratio between the measured [CH_4] in seawater to the calculated solubility in equilibrated seawater determines the supersaturation factor.

TCD
8, 121–147, 2014

2.3 CH_4 in bulk ice and brine

We used the wet extraction method to extract CH_4 from sea ice, as described in Raynaud et al. (1982) for continental ice. Briefly, 80 g of ice sample were put in a small container, using a 5 cm vertical resolution. The ice sample was then melted in the container under vacuum (10^{-3} torr), using a "bain-marie". It was then slowly refrozen from the bottom, using an ethanol (96 %) bath that was cooled to −80 °C by addition of liquid N_2. After refreezing, the whole gas content (both dissolved and in the bubbles) was expelled to the headspace of the container. The expelled gas was then injected, through a 22 mL packed column (Mole Sieve 5 A 80/100; 5 m × 1/8″), into a gas chromatograph (Trace GC) equipped with a flame ionisation detector for [CH_4] measurement. The reproducibility of the measurement, based on triplicate analysis of 5 different standards, was 99.6 %.

The method described here above gives [CH_4] in bulk ice. Providing that there is no CH_4 in the pure ice matrix, and hence that the entire amount of CH_4 (dissolved or in gas bubbles) is found within the ice pores (i.e. brine channels), [CH_4] bulk ice multiplied by the brine volume fraction (Cox and Weeks, 1983) gives the deduced [CH_4] in brine.

Dissolved [CH_4] in brine was also measured on brine samples collected using the sackhole technique. Sackholes were drilled at different depths, ranging from 20 to 130 cm. Brines, from adjacent brine channels and pockets, seeped into the sackholes and were collected after 10 to 60 min using a peristaltic pump (Cole Palmer, Masterflex® – Environmental Sampler). Each sackhole remained covered with a plastic lid to minimize mixing with the free-atmosphere. Brines were collected in 70 mL glass serum bottles, filled to overflowing, poisoned with 100 µL of saturated $HgCl_2$ and sealed with butyl stoppers and aluminium caps. The measured [CH_4] in brine is an integrated value of the CH_4 in brine from all the ice layers above the sampling depth. Therefore, the vertical resolution is lower than that of the [CH_4] in brine that is deduced from the [CH_4] in bulk ice. It is also noteworthy that the relative contribution of the various depth levels is unknown and dependent on the brine volume changes with depth. However,

TCD
8, 121–147, 2014

it is of interest to compare the measured $[CH_4]$ in brine with the $[CH_4]$ in brine that is deduced from the bulk ice values, as discussed later on.

For data interpretation, we calculated CH_4 solubility in brine and in ice (i.e., potential $[CH_4]$ dissolved in brine and in bulk ice, respectively). The solubility of CH_4 in brine was calculated using the temperature and salinity-dependent solubility of Wiesenburg and Guinasso (1979) as for seawater. This is allowed providing that the relationship of Wiesenburg and Guinasso (1979) is valid for the ranges of brine-temperature and -salinity. As for the conversion of $[CH_4]$ in bulk ice into the deduced $[CH_4]$ in brine, we simply divided the solubility of CH_4 in brine by the brine volume ratio to get the solubility of CH_4 in bulk ice. Brine salinity and brine volume (used in the calculations) were derived from the relationship of Cox and Weeks (1983). The ratio between the observed $[CH_4]$ in ice or brine to their respective calculated solubility determines the supersaturation factor.

In addition, to quantify the amount of CH_4 within the ice cover, we computed the standing stock of CH_4, i.e. we integrated the concentrations of CH_4 in bulk ice vertically to obtain the CH_4 content per square meter of ice.

For further comparison with the literature, we also computed CH_4 mixing ratio. It is usually obtained by dividing the number of moles of CH_4 by the total gas content. However, since we did not measure the total gas content, we used instead the sum of atmospheric-dominant gases (O_2, N_2 and Ar, data not shown).

3 Results

3.1 CH_4 concentration in ice

$[CH_4]$ in bulk ice ranged between 3.4 nmol L_{ice}^{-1} and 17.2 nmol L_{ice}^{-1}. Mean $[CH_4]$ and standard deviation increased from BRW2 (6.4 ± 2.9 nmol L_{ice}^{-1}) to BRW7 (7.8 ± 3.3 nmol L_{ice}^{-1}) and decreased to 5.5 ± 1.5 nmol L^{-1} at BRW10. This evolution parallels that of the standing stocks of $[CH_4]$ which increased from BRW2 (5070 to 5430 nmol m^{-2}) to BRW7

TCD
8, 121–147, 2014

(9200 nmol m^{-2}), then decreased at BRW10 (7580 nmol m^{-2}) (Fig. 2). For data interpretation, sea ice thickness is also shown in Fig. 2. It appears that the mean [CH_4] and the standing stock increased as sea ice thickened from BRW2 to BRW7, but decreased at BRW10 despite the fact that sea ice was thicker there.

The individual profiles of [CH_4] in bulk ice (Fig. 3a) for each sampling event further highlight the contrasts between BRW10 and all the previous sampling events (BRW2 to BRW7): all the [CH_4] profiles in ice from BRW2 to BRW 7 can be divided into 3 main zones. The first one ranged from 0 to 25 cm, where a peak of [CH_4] was found at 15 to 25 cm. [CH_4] measurements made on a twin ice core of BRW2 (duplicate) show that spatial variability in the layer of 15 to 25 cm could reach 60 %. The second zone was found in the ice interior, and ranged from 25 cm to the upper limit of the permeable layers (shaded area), where [CH_4] were close to 5 nmol L_{ice}^{-1}. The third zone corresponds to the permeable layers where [CH_4] increased again toward the sea ice bottom, with values ranging between 5 to 10 nmol L_{ice}^{-1}. At BRW10, as the whole ice cover became permeable (shaded area at all depths), the whole profile flattened: the peak of [CH_4] around 15 to 25 cm disappeared, the ice interior still has a baseline at 5 nmol L_{ice}^{-1} and the increase of [CH_4] at the bottom is less obvious than in the previous sampling events.

Beside the strong vertical variation, [CH_4] in bulk ice were always higher than the solubility values in surface seawater that would have been in equilibrium with the atmosphere (3.8 nmol L_{sw}^{-1}) and the theoretical solubility in ice at all depths (Fig. 3a – white dots). [CH_4] in bulk ice were in average 1.8 times higher than that in surface seawater and 75 times higher than the theoretical solubility in ice. The highest supersaturation factor reached 396 and was measured in BRW6, at 20 to 25 cm depth. Again, BRW10 differs from all the other sampling events, with lower supersaturation factor (mean supersaturation and standard deviation were 11 ± 4 vs. 86 ± 68 for BRW2 to BRW7).

CH_4 mixing ratio (not shown) was also measured for BRW2, BRW4, BRW7 and BRW10. It ranged between 5.8 and 105.3 ppmV. The maximum mixing ratio was found

TCD
8, 121–147, 2014

in BRW4, at 15 to 20 cm depth; this is 3.6 times higher than the mean mixing ratio of 29 ppmV.

To summarize, BRW10 differs from all the other samplings events by its lower mean $[CH_4]$ and its flatter $[CH_4]$ profiles. Although all the ice samples were supersaturated relative to the ice and surface seawater, larger supersaturations were observed from BRW2 to BRW7 (less permeable ice cores) compared to BRW10 (entirely permeable ice core), especially at 15 to 25 cm depth where both $[CH_4]$ and CH_4 mixing ratio were found to be the highest.

3.2 CH_4 concentration in brine

Deduced $[CH_4]$ in brine ranged between 13.2 nmol L_{br}^{-1} and 677.7 nmol L_{br}^{-1}. These are thus much higher than the range of $[CH_4]$ measured in brine (10.0 to 36.2 nmol L_{br}^{-1}) (Fig. 3 – triangles) and in seawater (25.9 and 116.4 nmol L_{sw}^{-1}).

The evolution of $[CH_4]$ in brine across seasons was rather similar to that of $[CH_4]$ in bulk ice, except in the bottom layers. Indeed, from BRW2 to BRW7, high $[CH_4]$ in brine were also observed at 15 to 20 cm depth; but from that level, $[CH_4]$ in brine decreased and reached the lowest values at the sea ice bottom, where it is similar to CH_4 solubility in seawater. There was thus no slight increase of $[CH_4]$ in brine, as observed in the $[CH_4]$ in bulk ice, at the sea ice bottom. The profile of $[CH_4]$ in brine flattened at BRW10, with values ranging between 13.2 and 87.0 nmol L_{br}^{-1}, which are less variable and much closer to both the solubility values in brine and the actual measured $[CH_4]$ in brine than the ranges of values in the previous sampling events (35.6 nmol L_{br}^{-1} and 677.7 nmol L_{br}^{-1}). The minimum of $[CH_4]$ in brine was calculated at 12.5 cm. Temperature data was missing at the very surface, so that we could not compute $[CH_4]$ in brine above 12.5 cm.

TCD
8, 121–147, 2014

3.3 CH_4 concentration in seawater

Measured [CH_4] in seawater ranged between 25.9 and 116.4 nmol L_{sw}^{-1} (Fig. 3c). This is 7 to 31 times higher than seawater in equilibrium with the atmosphere (3.8 nmol L^{-1} for a salinity of 35 at 0°C) (Wiesenburg and Guinasso, 1979).

Measurements of [CH_4] in seawater were homogenous in time from BRW2 to BRW7, with a mean value and standard deviation of 42.0 ± 2.4 nmol L_{sw}^{-1} for BRW2 and 37.5 ± 6 nmol L_{sw}^{-1} for BRW 4 to BRW7. They then increased at all depths, at BRW10 and reached a mean value and standard deviation of 77.4 ± 27.8 nmol L_{sw}^{-1}.

4 Discussion

The present paper aims at understanding the physical controls on the [CH_4] in sea ice. Discussing the physical controls only makes sense if the variations of [CH_4] due to biological activities are negligible compared to those due to physical processes. Therefore, we will first assess the importance of biological activities on the variation of [CH_4] (Sect. 4.1), before discussing the physical controls on the profiles of [CH_4] in sea ice and brine (Sect. 4.2).

4.1 Impact of biological activities on [CH_4] in impermeable ice

To assess the impact of biological activities on [CH_4], we recalculated the standing stocks of BRW4 to BRW7 (Fig. 3), by considering only the 25 to 80 cm-depth layers. These choices are motivated by the following reasons: First, we suggest focusing on the standing stocks of the impermeable layers (i.e. layers that have a brine volume fraction below 5 % (Golden et al., 1998); layers above the shaded areas on Fig. 3a and b). These layers are considered as a closed system in terms of brine dynamics and are therefore suitable to assess biological transformation of CH_4. Second, we felt it appropriate to ignore the upper layer (0 to 25 cm), since spatial variability could be important

TCD
8, 121–147, 2014

in these layers (up to 60 % from 15 to 25 cm depth) as shown in Fig. 3a – BRW2. Third, we only focused on the sampling events that were collected at short time intervals (3 or 4 days), i.e., BRW4 to BRW7, rather than between BRW2 and BRW4 (56 days). This is mainly due to the similar physical properties of the ice cores collected at short-time-intervals (i.e., in terms of ice core length, ice temperature, ice salinity profiles).

Deduced CH_4 standing stocks were relatively stable among the samplings, with mean and standard deviation of $3086.7 \pm 42.5\,nmol\,m^{-2}$. We performed an ANOVA test on the standing stocks and differences between the samplings were not significant enough to exclude the possibility of random sampling variability. Therefore, we can conclude that biological production and consumption of CH_4 (if existent) was negligible in comparison with the amount of CH_4 that was physically incorporated in the impermeable ice layers. Dividing the standing stocks of BRW4, BRW6, BRW7 by the thickness of the impermeable layer (55 cm), we obtained a mean and standard deviation of $55.7 \pm 0.3\,nmol\,m^{-2}\,cm^{-1}$, which is the amount of CH_4 that was ultimately trapped in sea ice (incorporation minus vertical transport) for each centimetre of ice growth over an area of one square meter, in April (late growth period).

4.2 The mechanisms of CH_4 incorporation, enrichment and dilution in sea ice

4.2.1 Range of CH_4 in sea ice and seawater, comparison with the literature

Our [CH_4] in sea ice (3.4–17.2 $nmol\,L_{ice}^{-1}$) were slightly lower than those of Lorenson and Kvenvolden (1995) (15 $nmol\,L_{ice}^{-1}$ to 40 $nmol\,L_{ice}^{-1}$). The deduced mixing ratios (5.8 ppmV to 105.3 ppmV) were however much lower than the 11 000 ppmV of Shakhova et al. (2010). We attribute the observed differences to (1) [CH_4] in seawater and (2) ebullition processes (i.e., the seepage of CH_4 bubbles from the seafloor and their rising through the water column).

First, our [CH_4] in seawater (25.9 and 116.4 $nmol\,L_{sw}^{-1}$) are consistent with those reported in northern Alaska (10.7 $nmol\,L_{sw}^{-1}$ to 111.8 $nmol\,L_{sw}^{-1}$, Kvenvolden et al., 1993)

TCD
8, 121–147, 2014

and shallow shelf areas with CH_4 release from sediment and/or destabilized gas hydrate (2.1 nmol L_{sw}^{-1} to 154 nmol L_{sw}^{-1}, Shakhova et al., 2005), but are much lower than the measurements reported by Shakhova et al. (2010) (1.8 to 2880 nmol L_{sw}^{-1}). The differences in [CH_4] in seawater lead to contrasting CH_4 supersaturations (700 % and 3100 % in the present study vs. 100 % to 160 000 % in Shakhova et al., 2010). Assuming similar incorporation rates in both studies, lower CH_4 supersaturation in seawater leads to lower CH_4 incorporated into sea ice and hence lower CH_4 mixing ratio in sea ice.

Second, ebullition is a process associated with rapid bubble ascension, limiting gas equilibration with the surrounding water mass (Keller and Stallard, 1994). Therefore, in shallow locations, CH_4 bubbles released from the seafloor could reach the seawater surface (Keller and Stallard, 1994; McGinnis et al., 2006). We believe that ebullition could increase CH_4 at the sea ice–water interface and lead to larger CH_4 incorporation into sea ice than if the ebullition was absent. Ebullitions were clearly observed in the Siberian Arctic Shelf (Shakhova et al., 2010) and in that case, centimetre-size bubbles were found within the ice (Shakhova et al., 2010). Since we did not find any literature reporting ebullition processes at Barrow, and since our ice cores generally showed millimeter-size bubbles (Zhou et al., 2013), we believe that ebullition processes were much less important in our study are that those observed by Shakhova et al. (2010).

4.2.2 Mechanisms responsible for the vertical profile of [CH_4] in bulk ice and brine during ice growth

Although the CH_4 source was from seawater, [CH_4] in bulk ice from BRW2 to BRW7 did not show a C-shape profile, as would salinity for growing sea ice (Petrich and Eicken, 2010). Instead of a surface maximum for salt, we observed a sub-surface maximum for CH_4. We suggest three abiotic mechanisms to explain the vertical profile of [CH_4] in bulk ice: (1) gas escape during the initial ice growth phase in the surface layer (2)

TCD
8, 121–147, 2014

preferential gas accumulation in the sub-surface and (3) brine volume fraction effect for the bottom layer.

We believe that CH_4, similarly to CO_2, could escape from the ice to the atmosphere, at the beginning at the ice growth (Geilfus et al., 2013; Nomura et al., 2006). In addition, once sea ice is consolidated, changes in temperature and in the volume of brine pockets are likely to fracture the ice, causing the expulsion of brines (Notz and Worster, 2009) and air bubbles (Untersteiner, 1968) at the ice surface. These 2 processes could explain the decrease of [CH_4] in bulk ice at the very surface of sea ice (Fig. 3 and 4).

Preferential gas accumulation during ice growth has been described for argon (Ar) in (Zhou et al., 2013). Temperature and salinity changes in brine at sea ice formation lead to a sharp decrease of CH_4 solubility that favours bubble nucleation. Once formed, the bubbles migrate upward due to their buoyancy. They are blocked under the surface impermeable layer, leading to gas accumulation. Such process is supported by 2 characteristics: the presence of bubbles and large supersaturation (compared to the rest of the ice core). The presence of bubbles is suggested by the large difference between the deduced CH_4 in brine (which includes both CH_4 in bubbles and CH_4 that is dissolved in brine) (Fig. 3b, squares) and the actual measurements of CH_4 in brine (only CH_4 that is dissolved in brine) (Fig. 3, triangles). The largest CH_4 supersaturations relative to CH_4 solubility in ice were always found at 15 cm to 25 cm depth. Moreover, bubbles were observed through thin sections at the same depth and Ar showed supersaturation up to 2900 %, without disruption in the ice texture (Zhou et al., 2013). Therefore, the mechanism of preferential gas accumulation suggested for Ar may be relevant for CH_4 as well. Larger CH_4 supersaturation as compared to Ar supersaturation is likely due to the difference in CH_4 and Ar solubility; CH_4 that is less soluble would be more affected by temperature and salinity changes. It is also noteworthy that this process of bubble formation led to large variability as the duplicate of BRW2 showed up to 60 % of CH_4 variation at 15–25 cm depth.

As the freezing front progresses, the temperature gradient in the permeable layer reduces; bubble nucleation from solubility decrease is less efficient. As a consequence,

TCD
8, 121–147, 2014

CH_4 accumulates less and $[CH_4]$ in brine decrease towards the bottom. Such a decrease is however not observed for $[CH_4]$ in bulk ice. We attribute this to the brine volume fraction effect. Indeed, the higher the brine volume, the higher the number of moles contained in that volume, and hence the higher $[CH_4]$ in bulk ice. $[CH_4]$ in brine do not show the increase at the sea ice bottom because they have been normalized to the same brine volume fraction.

An alternative explanation to the preferential gas accumulation due to solubility changes would be that a direct bubble incorporation after a sudden but intense release of CH_4 bubbles from the sediment to the ice bottom. CH_4 release from sediment is possible since our $[CH_4]$ in seawater are consistent with that found in areas where CH_4 release from sediment and/or gas hydrate destabilization likely occur (see Sect. 4.2.1). However, this process does not explain the slow decrease of $[CH_4]$ in brine from 15–25 cm depth to the sea ice bottom (Fig. 3b), and we may also wonder why the ebullition only occurred once during the whole sampling period.

The efficiency of bubble formation in the retention of CH_4 in sea ice is assessed in Fig. 4. We calculated the ratio between CH_4 in ice and the CH_4 in seawater at BRW2 (44 nmol L_{sw}^{-1}), and the ratio between brine salinity and the salinity of seawater at BRW2 (32), at each ice depth, for all the sampling events. The CH_4 in seawater and the salinity of seawater of BRW2 were chosen as references for consistency with Zhou et al. (2013). Similar apparent fractionation means that CH_4 is retained (incorporated and transported) in sea ice in the same way to salt, while a difference in the apparent fractionation means a difference if their retention. Four main observations can be made. First, the apparent fractionation averaged 15 % but never reached 100 %. This is due to the rejection of impurities during sea ice formation (Weeks, 2010). Our study therefore suggests that sea ice rejects about 85 % of its impurities, but retains 15 % of them. This is in agreement with Petrich and Eicken (2010) suggesting that sea ice brine allows a retention of 10 to 40 % of seawater ions in the ice. Second, the highest apparent fractionation of CH_4 (up to 39 %) was observed at 15 to 25 cm-depth; in that layer, the retention of CH_4 could be higher than that of salt by a factor of 2. This supports the

TCD
8, 121–147, 2014

previous suggestion about preferential gas accumulation: the presence of gas bubbles allows higher retention of CH_4 than salt. Third, the apparent fractionation of CH_4 was lower than that of salt at the surface of all the sampling events, except at BRW10. We believe that these are related to the formation of some cracks at the ice surface (during the cold period) which have allowed gas to escape from sea ice to the atmosphere, as explained earlier in this section. The lower [CH_4] in bulk ice at these sampling events (Fig. 3a) tends to support the conjecture of gas escape. Four, below the top layer of about 25 cm of ice, both CH_4 and salt enrichment values are similar, indicating that in these ice layers, CH_4 should be mainly incorporated in the dissolved state, as salt is.

4.2.3 Sea ice permeability controls [CH_4] in bulk ice and brine during sea ice decay

At BRW10, both [CH_4] in bulk ice and deduced [CH_4] in brine decreased and became less variable than the previous samplings (BRW2 to BRW7). In addition, CH_4 standing stocks decreased by ca. 1600 nmol m^{-2} from BRW7 to BW10, and the deduced [CH_4] in brine became closer to the measured [CH_4] in brine. These measurements suggest an enhanced gas transport through the ice and that gas bubbles have escaped from sea ice to the atmosphere. Gas escape was allowed given that sea ice was permeable at all depths (Fig. 3a and b – shaded area). Concomitant Ar bubble escape was suggested in (Zhou et al., 2013). However, in contrast to Ar that was then at saturation, CH_4 was still supersaturated compared to the solubility in brine. This could be related to a slow exchange between the atmosphere, brine and the supersaturated seawater through diffusion.

[CH_4] in brine at BRW10 (13.2 nmol L_{br}^{-1} to 87.0 nmol L_{br}^{-1}) ranged between [CH_4] at ice/water interface (116.4 nmol L_{sw}^{-1}) and the theoretical [CH_4] in surface seawater that is in equilibrium with the atmosphere (3.8 nmol L_{sw}^{-1}). Although [CH_4] in brine at the very surface (0–12.5 cm) could not be retrieved, we can hypothesize that the gradient of [CH_4] between the ice/seawater interface and the ice surface led to CH_4 diffusion from

TCD
8, 121–147, 2014

ice/seawater interface to the ice surface, and therefore maintained [CH_4] supersaturated in ice, after gas bubble escape. Since the source of [CH_4] was from supersaturated seawater, [CH_4] in brine was slightly higher at the sea ice bottom than at the top.

5 Conclusions and perspectives

We reported on [CH_4] evolution in landfast sea ice and in under-ice water from February through June 2009 at Barrow (Alaska). [CH_4] in sea ice and [CH_4] in seawater are consistent with records from the area with CH_4 release from sediment and gas hydrate destabilization (Kvenvolden et al., 1993; Lorenson and Kvenvolden, 1995; Shakhova et al., 2010).

Gas exchange likely took place during initial ice growth between sea ice and the atmosphere, and the formation of cracks could lead to a decrease of CH_4 at the very surface of the ice. Then when sea ice reached ca. 25 cm of ice thickness, gas bubble formation triggered by strong solubility changes could have favoured CH_4 accumulation in ice. CH_4 retention in the ice was twice as efficient as that of salt. However, as sea ice thickens, CH_4 appeared to be trapped in the dissolved state, as salt does. We believe that the subsequent evolution of [CH_4] in impermeable sea ice layers mainly depends on physical processes, as [CH_4] did not seem to be affected by biological processes in these layers. Abrupt changes in [CH_4] in sea ice occur, associated with the release of gas bubbles to the atmosphere, when sea ice became permeable. Therefore, the main role of sea ice in the exchange of CH_4 from seawater to the atmosphere seems to be its control on the amount of CH_4 that it is able to store in its impermeable layers and the duration of such storage.

CH_4 dynamics in the permeable layers on sea ice decay need further investigation, since both physical processes (convection and diffusion) and biological processes may affect the [CH_4]. The implementation of gas component in sea ice biogeochemical models may help in studying these interactions. Additional methane oxidation measure-

TCD
8, 121–147, 2014

ment, incubation experiments, gene and isotopic studies should also help in deciphering the processes at work. Indeed, not all microorganisms are able to transform CH_4, and therefore the detection of methanogens and methanotrophs are a prerequisite in the study of CH_4 transformation in sea ice. If the behaviour of such microorganisms in ice is similar to those living in seawater, CH_4 production and consumption are both theoretically possible in anoxic micro-niches (Rysgaard and Glud, 2004) or in oxic brine channels, from DMSP degradation (Damm et al., 2010). Isotopic studies will provide additional evidence, since biogenic CH_4 within anoxic sediments has very negative carbon isotopic values: −50 % to −70 % (Brooks et al., 1991; Kvenvolden, 1995; Valentine et al., 2001), compared to that formed by CH_4 oxidation (−10 % to −24 %, Damm et al., 2008; Schubert et al., 2011).

Acknowledgements. The authors would like to thank Hajo Eicken, the rest of the sea ice group of the Geophysical Institute of the University of Alaska Fairbanks, Tim Papakyriakou, Bernard Heinesch, Michel Yernaux, Frédéric Brabant, Thomas Goossens, Noémie Carnat and Rodd Laing for their help in field work. We are indebted to the Barrow Arctic Science Consortium and the North Slope Borough for their logistical support. We also thank Saïda El Amri and Arnaud Rottier for their efficient help in laboratory work, Ceri Middleton for language help and Neige Egmont for her comments. This research was supported by the F.R.S-FNRS (contract 2.4584.09), the National Science Foundation (project OPP-0632398 (SIZONet)), the University of Alaska Fairbanks and the Belgian Science Policy (contract SD/CA/03A), the NCE ArcticNet and National Science and Engineering Research Council (NSERC). NXG received a PhD grant from F.R.S.-FRIA. J. Zhou is a research fellow of F.R.S.-FNRS, B. Delille is a research associate of F.R.S.-FNRS. This is a MARE contribution.

References

Abril, G. and Iversen, N.: Methane dynamics in a shallow non-tidal estuary (Randers Fjord, Denmark), Mar. Ecol.-Prog. Ser., 230, 171–181, 2002.

Bange, H. W., Bartell, U. H., Rapsomanikis, S., and Andreae, M. O.: Methane in the Baltic and North Seas and a Reassessment of the Marine Emissions of Methane, Global Biogeochem. Cy., 8, 465–480, 1994.

TCD
8, 121–147, 2014

Bates, T. S., Kelly, K. C., Johnson, J. E., and Gammon, R. H.: A reevaluation of the open ocean source of methane to the atmosphere, J. Geophys. Res., 101, 6953–6961, 1996.
Borges, A. V. and Abril, G.: 5.04 – Carbon dioxide and methane dynamics in estuaries, in: Treatise on Estuarine and Coastal Science, edited by: Eric, W. and Donald, M., Academic Press, Waltham, 2011.
Brooks, J. M., Field, M. E., and Kennicutt, M. C.: Observations of gas hydrates in marine-sediments, offshore Northern California, Mar. Geol., 96, 103–109, 1991.
Cox, G. F. N. and Weeks, W. F.: Equations for determining the gas and brine volumes in sea-ice samples, J. Glaciol., 29, 306–316, 1983.
Damm, E., Schauer, U., Rudels, B., and Haas, C.: Excess of bottom-released methane in an Arctic shelf sea polynya in winter, Cont. Shelf Res., 27, 1692–1701, 2007.
Damm, E., Kiene, R. P., Schwarz, J., Falck, E., and Dieckmann, G.: Methane cycling in Arctic shelf water and its relationship with phytoplankton biomass and DMSP, Mar. Chem., 109, 45–59, 2008.
Damm, E., Helmke, E., Thoms, S., Schauer, U., Nöthig, E., Bakker, K., and Kiene, R. P.: Methane production in aerobic oligotrophic surface water in the central Arctic Ocean, Biogeosciences, 7, 1099–1108, doi:10.5194/bg-7-1099-2010, 2010.
Florez-Leiva, L., Damm, E., and Farías, L.: Methane production induced by dimethylsulfide in surface water of an upwelling ecosystem, Prog. Oceanogr., 112–113, 38–48, doi:10.1016/j.pocean.2013.03.005, 2013.
Forster, P., Ramaswamy, V., Artaxo, P., Berntsen, T., Betts, R., Fahey, D. W., Haywood, J., Lean, J., Lowe, D. C., Myhre, G., Nganga, J., Prinn, R., Raga, G., Schulz, M., and Dorland, R. V.: Changes in atmospheric constituents and in radiative forcing, in: Climate Change 2007: The Physical Science Basis. Contribution of Working Group I to the Fourth Assessment Report of the Intergovernmental Panel on Climate Change, edited by: Solomon, S., Qin, D., Manning, M., Chen, Z., Marquis, M., Averyt, K. B., M.Tignor, and Miller, H. L., Cambridge University Press, Cambridge, UK, 2007.
Geilfus, N. X., Carnat, G., Papakyriakou, T., Tison, J. L., Else, B., Thomas, H., Shadwick, E., and Delille, B.: Dynamics of pCO_2 and related air–ice CO_2 fluxes in the Arctic coastal zone (Amundsen Gulf, Beaufort Sea), J. Geophys. Res.-Oceans, 117, C00G10, doi:10.1029/2011JC007118, 2012.
Geilfus, N. X., Carnat, G., Dieckmann, G. S., Halden, N., Nehrke, G., Papakyriakou, T., Tison, J. L., and Delille, B.: First estimates of the contribution of $CaCO_3$ precipitation to the

TCD
8, 121–147, 2014

release of CO_2 to the atmosphere during young sea ice growth, J. Geophys. Res.-Oceans, 118, 244–255, doi:10.1029/2012JC007980, 2013.
Golden, K. M., Ackley, S. F., and Lytle, V. I.: The percolation phase transition in sea ice, Science, 282, 2238–2241, 1998.
He, X., Sun, L., Xie, Z., Huang, W., Long, N., Li, Z., and Xing, G.: Sea ice in the Arctic Ocean: role of shielding and consumption of methane, Atmos. Environ., 67, 8–13, 2013.
Judd, A. G.: Natural seabed gas seeps as sources of atmospheric methane, Environ. Geol., 46, 988–996, 2004.
Karl, D. M., Beversdorf, L., Bjorkman, K. M., Church, M. J., Martinez, A., and DeLong, E. F.: Aerobic production of methane in the sea, Nat. Geosci., 1, 473–478, 2008.
Keller, M. and Stallard, R. F.: Methane emission by bubbling from Gatun Lake, Panama, J. Geophys. Res., 99, 8307–8319, 1994.
Kennett, J. P., Cannariato, K. G., Hendy, I. L., and Behl, R. J.: Carbon isotopic evidence for methane hydrate instability during quaternary interstadials, Science, 288, 128–133, 2000.
Kitidis, V., Upstill-Goddard, R. C., and Anderson, L. G.: Methane and nitrous oxide in surface water along the North-West Passage, Arctic Ocean, Mar. Chem., 121, 80–86, 2010.
Kort, E. A., Wofsy, S. C., Daube, B. C., Diao, M., Elkins, J. W., Gao, R. S., Hintsa, E. J., Hurst, D. F., Jimenez, R., Moore, F. L., Spackman, J. R., and Zondlo, M. A.: Atmospheric observations of Arctic Ocean methane emissions up to 82° north, Nat. Geosci., 5, 318–321, 2012.
Kvenvolden, K.: Natural-gas hydrate occurrence and issues, Sea. Technol., 36, 69–74, 1995.
Kvenvolden, K., Lilley, M. D., and Lorenson, T. D.: The Beaufort Sea Continental Shelf as a seasonal source of atmospheric methane, Geophys. Res. Lett., 20, 2459–2462, 1993.
Lawrence, D. M., Slater, A. G., Tomas, R. A., Holland, M. M., and Deser, C.: Accelerated Arctic land warming and permafrost degradation during rapid sea ice loss, Geophys. Res. Lett., 35, L11506, doi:10.1029/2008GL033985, 2008.
Lelieveld, J., Crutzen, P. J., and Dentener, F. J.: Changing concentration, lifetime and climate forcing of atmospheric methane, Tellus B, 50, 128–150, 1998.
Loose, B., McGillis, W. R., Schlosser, P., Perovich, D., and Takahashi, T.: Effects of freezing, growth, and ice cover on gas transport processes in laboratory seawater experiments, Geophys. Res. Lett., 36, L05603, doi:10.1029/2008GL036318, 2009.

TCD
8, 121–147, 2014

Lorenson, T. D. and Kvenvolden, K. A.: Methane in coastal sea water, sea ice, and bottom sediments, Beaufort Sea, Alaska, U.S. Geological Survey Open-File Report 95-70, U.S. Geological Survey, Menlo Park, CA, 1995.

McGinnis, D. F., Greinert, J., Artemov, Y., Beaubien, S. E., and Wüest, A.: Fate of rising methane bubbles in stratified waters: how much meane reaches the atmosphere?, J. Geophys. Res., 111, C09007, doi:10.1029/2005JC003183, 2006.

Nisbet, E. G.: Have sudden large releases of methane from geological reservoirs occurred since the Last Glacial Maximum, and could such releases occur again?, Philos. T. Roy. Soc. A, 360, 581–607, 2002.

Nomura, D., Yoshikawa-Inoue, H., and Toyota, T.: The effect of sea-ice growth on air–sea CO_2 flux in a tank experiment, Tellus B, 58, 418–426, 2006.

Nomura, D., Eicken, H., Gradinger, R., and Shirasawa, K.: Rapid physically driven invesrion of the air–sea ice CO_2 flux in the seasonal landfast ice off Barrow, Alaska after onset of surface melt, Cont. Shelf Res., 30, 1998–2004, 2010.

Notz, D. and Worster, M. G.: Desalination processes of sea ice revisited, J. Geophys. Res., 114, C05006, doi:10.1029/2008JC004885, 2009.

Petrich, C. and Eicken, H.: Growth, structure and properties of sea ice, in: Sea Ice, edited by: Thomas, D. N. and Dieckmann, G. S., Blackwell Publishing Ltd, UK, 2010.

Raynaud, D., Delmas, R., Ascencio, J. M., and Legrand, M.: Gas extraction from polar ice cores: a critical issue for studying the evolution of atmospheric CO_2 and ice-sheet surface elevation, Ann. Glaciol., 3, 265–268, 1982.

Reagan, M. T. and Moridis, G. T.: Dynamic response of oceanic hydrate deposits to ocean temperature change, J. Geophys. Res., 113, C12023, doi:10.1029/2008JC004938, 2008.

Romanovskii, N. N., Hubberten, H. W., Gavrilov, A. V., Tumskoy, V. E., Tipenko, G. S., Grigoriev, M. N., and Siegert, C.: Thermokarst and land-ocean interactions, Laptev Sea Region, Russia, Permafrost. Periglac., 11, 137–152, 2000.

Rysgaard, S. and Glud, R. N.: Anaerobic N_2 production in Arctic sea ice, Limnol. Oceanogr., 49, 86–94, 2004.

Savvichev, A. S., Rusanov, I. I., Yusupov, S. K., Pimenov, N. V., Lein, A. Y., and Ivanov, M. V.: The biogeochemical cycle of methane in the coastal zone and littoral of the Kandalaksha Bay of the White Sea, Microbiology, 73, 457–468, 2004.

TCD
8, 121–147, 2014

Schubert, C. J., Vazquez, F., Lösekann-Behrens, T., Knittel, K., Tonolla, M., and Boetius, A.: Evidence for anaerobic oxidation of methane in sediments of a freshwater system (Lago di Cadagno), FEMS Microbiol. Ecol., 76, 26–38, 2011.
Shakhova, N., Semiletov, I., and Panteleev, G.: The distribution of methane on the Siberian Arctic shelves: implications for the marine methane cycle, Geophys. Res. Lett., 32, L09601, doi:10.1029/2005GL022751, 2005.
Shakhova, N., Semiletov, I., Salyuk, A., Yusupov, V., Kosmach, D., and Gustafsson, O.: Extensive methane venting to the atmosphere from sediments of the East Siberian Arctic shelf, Science, 327, 1246–1250, 2010.
Skoog, D. A., West, D. M., and Holler, F. J.: Chimie Analytique, De Boeck Université, Paris, Bruxelles, 1997.
Untersteiner, N.: Natural desalinisation and equilibrium salinity profile of perennial sea ice, J. Geophys. Res., 73, 1251–1257, 1968.
Upstill-Goddard, R. C., Barnes, J., Frost, T., Punshon, S., and Owens, N. J. P.: Methane in the southern North Sea: low-salinity inputs, estuarine removal, and atmospheric flux, Global Biogeochem. Cy., 14, 1205–1217, 2000.
Valentine, D. L., Blanton, D. C., Reeburgh, W. S., and Kastner, M.: Water column methane oxidation adjacent to an area of active hydrate dissociation, Eel River Basin, Geochim. Cosmochim. Ac., 65, 2633–2640, 2001.
Weeks, W. F.: On Sea Ice, University of Alaska Press, Fairbanks, Alaska, 2010.
Westbrook, G. K., Thatcher, K. E., Rohling, E. J., Piotrowski, A. M., Pälike, H., Osborne, A. H., Nisbet, E. G., Minshull, T. A., Lanoisellé, M., James, R. H., Hühnerbach, V., Green, D., Fisher, R. E., Crocker, A. J., Chabert, A., Bolton, C., Beszczynska-Möller, A., Berndt, C., and Aquilina, A.: Escape of methane gas from the seabed along the West Spitsbergen continental margin, Geophys. Res. Lett., 36, L15608, doi:10.1029/2009GL039191, 2009.
Wiesenburg, D. A. and Guinasso, N. L.: Equilibrium solubilities of methane, carbon monoxide and hydrogen in water and sea water, J. Chem. Eng. Data, 24, 356–360, 1979.
Yamamoto, S., Alcauskas, J. B., and Crozier, T. E.: Solubility of methane in distilled water and seawater, J. Chem. Eng. Data, 21, 78–80, 1976.
Zeikus, J. G. and Winfrey, M. R.: Temperature limitation of methanogenesis in aquatic sediments, Appl. Environ. Microb., 31, 99–107, 1976.
Zhou, J., Delille, B., Eicken, H., Vancoppenolle, M., Brabant, F., Carnat, G., Geilfus, N.-X., Papakyriakou, T., Heinesch, B., and Tison, J.-L.: Physical and biogeochemical properties in

TCD
8, 121–147, 2014

landfast sea ice (Barrow, Alaska): insights on brine and gas dynamics across seasons, J. Geophys. Res.-Oceans, 118, 3172–3189, 2013.

Zindler, C., Bracher, A., Marandino, C. A., Taylor, B., Torrecilla, E., Kock, A., and Bange, H. W.: Sulphur compounds, methane, and phytoplankton: interactions along a north–south transit in the western Pacific Ocean, Biogeosciences, 10, 3297–3311, doi:10.5194/bg-10-3297-2013, 2013.

TCD

8, 121–147, 2014

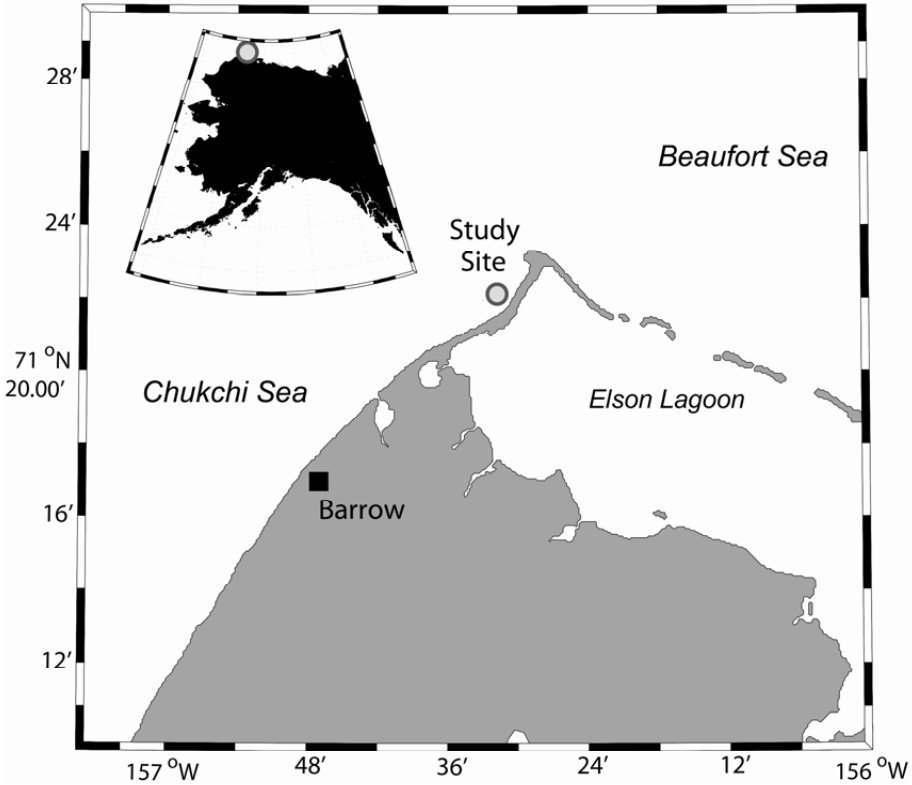

Fig. 1. The study site. North of Barrow, Alaska, US.

TCD
8, 121–147, 2014

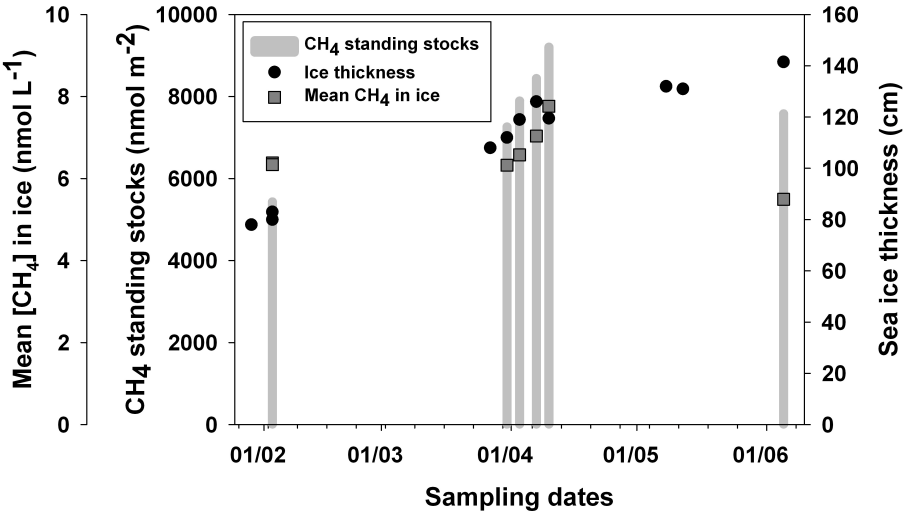

Fig. 2. CH_4 standing stocks for selected samplings events (vertical bars, from left to right, BRW2, BRW4, BRW5, BRW6, BRW7 and BRW10) in parallel with mean [CH_4] in sea ice and sea ice thickness.

TCD
8, 121–147, 2014

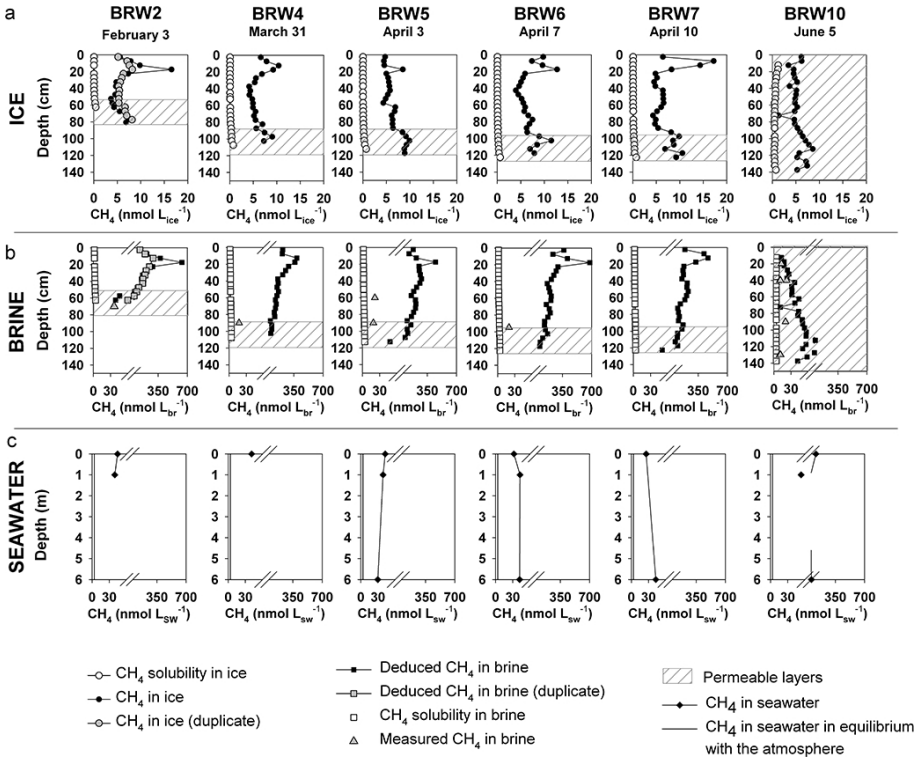

Fig. 3. Evolution of CH_4 concentration in **(a)** bulk ice, **(b)** brine and **(c)** seawater (black dots, squares and diamonds, respectively), compared to CH_4 solubility in ice, brine and seawater that is in equilibrium with the atmosphere (white dots, white squares and black straight lines, respectively). Grey dots and grey squares are measurements made on duplicate samples of BRW2. Grey triangles in **(b)** are CH_4 measurements in brine sackholes. The break in the *x* axes of **(b)** and **(c)** is set at 60 nmol L^{-1}. Dashed areas are permeable layers (i.e. layers with brine volume fraction above 5 %).

TCD
8, 121–147, 2014

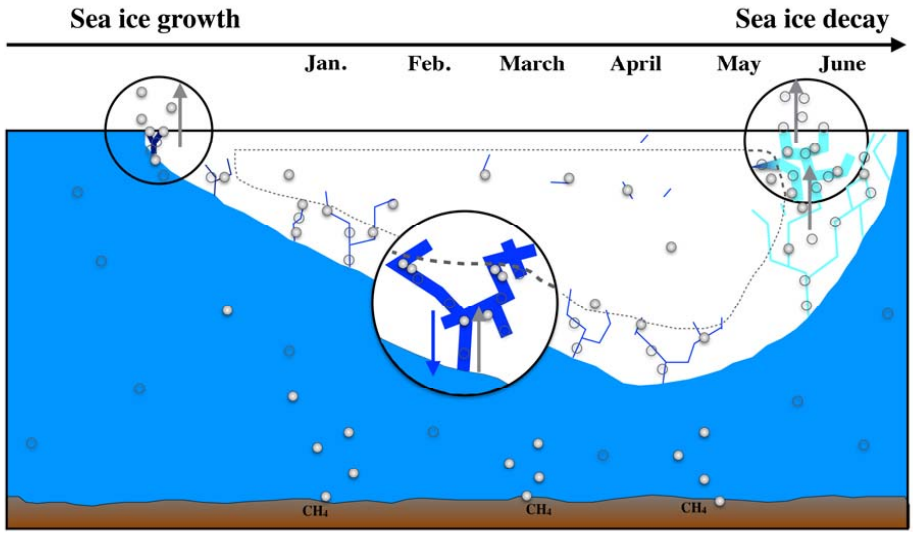

Fig. 4. Schematic figure of CH_4 release and incorporation in sea ice. Sizes are intentionally disproportionate to better highlight processes. The area within the closed dotted line represents the impermeable layers. The small filled and empty circles represent CH_4 in gas bubbles and in dissolved state respectively. Upward grey arrows indicate the upward transport of gas bubbles due to their buoyancy, while downward blue arrows indicate the removal of dissolved gas through brine drainage. Large black circles zoom on particular processes described in the text (Sect. 4.1): gas exchanges at the beginning of ice growth, preferential gas accumulation under the impermeable layers and gas bubble escape during ice decay. Dark blue, light blue and cyan strokes in ice represent brine channels with high, moderate or low salinity, respectively.

TCD
8, 121–147, 2014

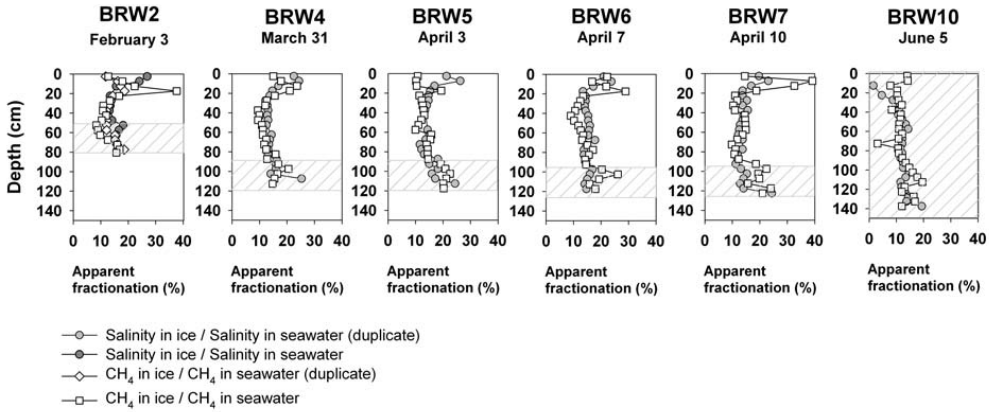

Fig. 5. Comparison between the apparent fractionation of salinity in ice (the ratio between ice salinity and the seawater salinity (32)) and the apparent fractionation of CH_4 (the ratio between CH_4 in ice and CH_4 in seawater (44 nmol L_{sw}^{-1})). The seawater salinity and CH_4 in seawater that are chosen as references were the values obtained from BRW2. Dashed areas are permeable layers (i.e. layers with brine volume fraction above 5 %).

TCD
8, 121–147, 2014